# Characterization and processing of blends of poly(ether imide) with thermotropic liquid crystalline polymer

**Sangmook Lee, Soon Man Hong, Yongsok Seo*, Tae Suk Park, Seung Sang Hwang and Kwang Ung Kim**
*Polymer Processing Laboratory, Korea Institute of Science and Technology (KIST), PO Box 131, Cheongryang, Seoul, Korea 130-650*

**and Jae Wook Lee**
*Department of Chemical Engineering, Sogang University, 1-1, Shinsudong, Mapokoo, Seoul, Korea 121-742*
*(Received 4 February 1993; revised 1 June 1993)*

We investigated thermal, rheological, morphological and mechanical properties of an *in situ* composite of poly(ether imide) (PEI) and thermotropic liquid crystalline polymer (TLCP). Ultem 1000 was used as a matrix and Vectra B950 was used as the *in situ* reinforcing TLCP. Fibre-spinning of the blends was performed on a capillary rheometer. Differential scanning calorimetry thermograms of extruded fibres indicated that the thermal properties of PEI did not change noticeably with the amount of TLCP but thermogravimetric analysis showed that thermal stability of the blend was decreased with the amount of TLCP. Immiscibility was checked with thermal data. The rheological properties of the blends changed remarkably with temperature and composition. The tensile strength and modulus of blend fibre increased with TLCP content and spin draw ratio. The increase of tensile strength was more striking for the fibre of the blend containing more TLCP. Wide angle X-ray patterns suggested that the increase in tensile strength was due to the enhanced molecular orientation and resultant fibrillation of TLCP. A modified Tsai–Halpin equation was used to predict the aspect ratio of microfibrils for these blends. Morphology of the blend showed that PEI/TLCP fibres contained fine fibrils of almost infinite aspect ratio and nearly perfect orientation in the flow direction. The draw ratio effect on the mechanical properties was remarkable at low draw ratio, but levelled off soon. The amount of TLCP influenced the fibril formation. Morphological observation showed the effect of thermal history of the blend and its effect on mechanical performance. The blend showed maximum aspect ratio and aspect ratio change when TLCP content was 25 wt%. TLCP orientation and its steric effect seem to induce the optimum TLCP amount for fibril formation.

**(Keywords: composite; poly(ether imide); morphology)**

## INTRODUCTION

The mechanical properties of polymers can be greatly enhanced by the addition of fibrous fillers. Thermoset composite is a typical example, whereas composites based on thermoplastics have been less successful. This is due mainly to numerous problems encountered during their processing and fabrication. As mentioned by Mithal *et al.*[1], the addition of fibres to polymer melt increases its viscosity substantially, leading to problems of quick freeze-off, poor mould filling, longer cycle times and increased power consumption. Increasing temperature to counterbalance viscosity may cause thermal degradation. Conflicting requirements of the compounding process, such as uniform dispersion and minimal fibre breakage, demand the careful balance of fibre aspect ratio, fibre size distribution and uniformity of the product. The compounding process in itself is an added expense. Moreover, abrasive wear on the processing equipment, due to surface hardness of the reinforcing fibres (particularly glass fibres), induces the need for early replacement. Thus the final product is the result of a series of compromises between product quality, fibre volume content and processability.

One possible way to circumvent these problems is to develop compositions that may be processed at elevated temperature as homogeneous melts from which a rigid reinforcing phase develops when the material is cooled. Liquid crystalline polymers (LCPs) generally exhibit lower viscosities than isotropic polymer melts. Thermotropic liquid crystalline polymers (TLCPs) have chain backbones with highly extended conformations; they can therefore be further orientated spontaneously under the influence of extensional flows, as in fibre spinning. Orientated LCPs relax very slowly due to the rotation of whole molecules or the cooperative motion of many molecular units. Therefore the orientation developed in a processed melt can be retained after solidification. These self-orientating fibrous inclusions then function as reinforcing elements. Thus, the liquid

* To whom correspondence should be addressed

0032-3861/94/030519-13

crystalline species can serve as a processing aid at elevated temperatures as well as a reinforcing fibre in the solid state. The composite made in this way is termed an '*in situ* composite'. Some interesting advantages of this *in situ* composite over conventional inorganic reinforced thermoplastic composites are: highly enhanced processability due to the low melt viscosity; uniform product properties resulting from better dispersion of reinforcements; and less equipment damages. Furthermore, detrimental mechanical properties originating from differences in thermal expansion coefficients between matrix polymer and reinforcement can be controlled easily. In addition to the processing advantage of *in situ* composites over macroscopic fibre-reinforced composites, they have a higher efficiency of fibre utilization. The strength of an isolated extended chain of molecules exceeds, by an order of magnitude or more, the strength of fibres produced from the same material[2]. Thus, the mechanical properties of isotropic polymers can be enhanced by the addition of TLCPs without resorting to fibre reinforcement.

TLCP, which is initially dispersed as spheres or droplets, can be elongated in adequate flow fields to give *in situ* reinforcement by forming fine fibrils with larger length and smaller diameter than glass fibres, for instance. Several TLCPs have been tested as reinforcing species for various isotropic polymer matrices of polystyrene[3–5], polycarbonate[6–12], poly(ether sulfone)[13,14], nylons[15–18], poly(ethylene terephthalate)[19–22], polysulfone[23], poly(phenylene sulfide)[24] and polyarylate[25].

Poly(ether imide) (PEI) is a speciality engineering thermoplastic resin, which marks a major breakthrough in improving heat and chemical resistance as well as flame resistance. It has high strength, high modulus, high glass transition temperature, and yet remains stable over a wide range of temperatures and frequencies. However, its normal processing temperature is quite high. PEI would be more desirable if it could be processed at lower temperature (less than 300°C). As part of our continuous effort to devise a highly thermally stable and mechanically strong composite with low processing temperature, we present the results of preliminary thermal, mechanical, morphological and rheological studies conducted on strands of PEI with TLCP, and elucidate the parameters that control the formation of these fibrils *in situ*.

## EXPERIMENTAL

### *Materials*

The TLCP used was an extrusion grade resin, Vectra B950, produced by Hoechst Celanese, which has a copolymer composition based on 6-hydroxy-2-naphthoic acid (58%), terephthalic acid (21%) and aminophenol (21%). The PEI used was an amorphous thermoplastic resin, Ulten 1000 purchased from General Electric Co.

### *Blending and fibre spinning*

The pellets of all materials used were dried in a vacuum oven at 120°C for at least 24 h before use. TLCP contents were 0, 5, 10, 25, 50, 75 and 100 wt%. Blends were made as follows. Dried pellets of Vectra B950 and Ultem were mixed in a container before blending in a counter-rotating internal mixer (Brabender PLE330) at 375°C. The melt was cooled and then pelletized in a pulverizer. The pellets were dried at 120°C for at least 24 h before fibre extrusion. The fibres were spun using a capillary rheometer (Instron 3211) with a capillary $L/D$ ratio of 40 and diameter of 1.27 mm. Draw ratio, defined as the ratio of die and the fibre diameter, was controlled by the speed of the take-up roll. The spinning temperature was between 300 and 340°C.

### *Mechanical properties*

Mechanical properties of the blends were tested using an Instron Universal Testing Machine (model 4204) at a constant temperature and humidity. A gauge length of 30 mm and a crosshead speed of 10 mm $min^{-1}$ were used. Each tensile property was averaged over 10 tests.

### *Morphology and fine structure*

Morphological observation was performed using a scanning electron microscope (Hitachi S-510). Fibre orientation was investigated using an X-ray diffractometer (Rigaku D). Spun fibres were fractured in liquid nitrogen. Samples for microscopy were coated with 10–15 nm of gold prior to analysis.

### *Rheological properties*

Rheological properties of the blends and pure resins were measured using a Rheometrics Dynamic Spectrometer (model RDS 7700) on which parallel plates with a diameter of 50 or 25 mm were mounted. The frequency range was set at 0.1–500 rad $s^{-1}$ and the applied strain was 10%. The plate gap was 1.2 mm. Before the test, the samples were prepared using a compression moulder at 350°C. Measurement was made under nitrogen atmosphere.

### *Thermal properties*

A Dupont 2000 thermal analyser was used for thermal characterization. The weight of all samples was 7–8 mg. The heating rate was 10°C $min^{-1}$ and the materials were scanned from 30 to 350°C. Following the first scan, the samples were quickly quenched at a cooling rate of 320°C $min^{-1}$ and reheated as the second run. A Dupont 2000 thermal gravimetric analyser was also used to observe the degradation of samples. The heating rate was 10°C $min^{-1}$ and samples were heated up to 800°C.

## RESULTS AND DISCUSSION

### *Thermal properties*

The results of d.s.c. heating scans for the PEI/TLCP blends are presented in *Figure 1*. As a highly heat resistant resin, PEI shows its glass transition temperature ($T_g$) at 217°C. TLCP has a relatively wide endothermic melting peak. Its transition to the nematic phase ($T_m$) appears at 278°C. The clearing temperature is well above the thermal decomposition temperature. We could not observe the $T_g$ of TLCP due to its small thermal heat capacity difference. Besides the major melting transition of TLCP at 279°C, a minor melting transition appears at around 288°C. The minor transition is attributed to the melting of highly ordered crystallites, which can persist above the major melting transition. This minor melting transition varies with the heating rate and the thermal history of the sample. TLCP already flows above the major melting transition temperature corresponding to the nominal $T_m$. Similar behaviour was observed for polyester LCP. The

**Table 1** Thermal properties of PEI/TLCP blends

| TLCP content (wt%) | $T_g$ (°C) | $T_m$ (°C) | $\Delta H_m$ (J g$^{-1}$) | $\Delta H_m$ (J/TLCPg) | $T_c$ (°C) | $\Delta H_c$ (J g$^{-1}$) | $\Delta H_c$ (J/TLCPg) |
|---|---|---|---|---|---|---|---|
| 0 | 217.3 | | | | | | |
| 5 | 215.5 | | | | | | |
| 10 | 216.8 | | | | | | |
| 25 | 211.3 | 274.7 | 0.57 | 2.28 | 229.9 | 0.13 | 0.52 |
| 50 | 213.3 | 278.1 | 1.19 | 2.39 | 229.7 | 0.25 | 0.50 |
| 75 | 210.8 | 276.6 | 1.80 | 2.39 | 230.7 | 0.56 | 0.75 |
| 100 | – | 279.0 | 2.31 | 2.31 | 230.7 | 1.53 | 1.53 |

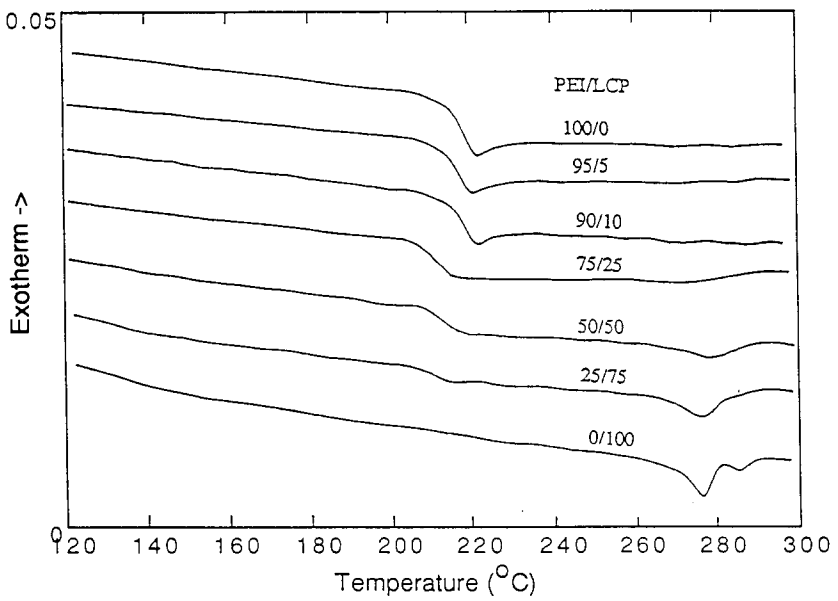


**Figure 1** D.s.c. thermograms of PEI/TLCP blends (heating rate 10°C min$^{-1}$)

presence of highly ordered crystallites in Vectra A900 (a random copolyester with 73 mol% hydroxybenzoic acid and 27 mol% 6-hydroxy-2-naphthoic acid) was found to have a severe influence on the stability of TLCP melt in the temperature range between the major and minor melting transitions[26].

Thermal properties of the blends are summarized in *Table 1*. Increasing the TLCP contents in the blends results in two different behaviours. The $T_g$ was close to 216.5°C up to a TLCP content of 25% in the blend, but above this content it fell to 212°C. This may be due to more active movement of the TLCP chains. The melting temperature ($T_m$) of TLCP did not vary with the increase in amount of TLCP, but the heat of nematic transition and heat of fusion per unit mass of TLCP ($\Delta H_m$) were increased. Also, the heat of crystallization ($\Delta H_c$) and crystallization temperature ($T_c$) were increased with TLCP content. This indicates that the degree of crystallinity of the blends was increased with the addition of TLCP. It also suggests that the PEI and TLCP (copolyesteramide) used in this study are almost incompatible in all the examined compositions. As already mentioned, pure TLCP shows two crystal–nematic transition peaks whereas the blends show only one transition peak which is ascribable to the hindrance of PEI to form highly orientated crystallites[26].

*Figure 2* shows the weight loss of PEI/Vectra B950 blends measured by thermogravimetric analysis (t.g.a.) under nitrogen atmosphere. The curves in *Figure 2* show that the thermal stability of the blends is decreased with increasing TLCP content, which means that the thermal stability of PEI is better than TLCP. *Table 2* summarizes dynamic thermogravimetric data. Decomposition onset temperature (*DOT*) is defined as the temperature at which 1% of the weight is lost. Maximum decomposition temperature (*MDT*) is the temperature of the maximum weight loss. *DOT* is a maximum when the TLCP content is 50%. It appears that the maximum instability occurs at this composition. This is similar to what Calahorra *et al.*[27] observed in polyarylate/poly(ethylene terephthalate) blends. *MDT* is decreased with increasing TLCP content. *Figure 3* shows the gradient of the weight loss *versus* temperature. The *MDT* peak occurs at around 550°C in pure PEI resin. The peak height slowly lessens with TLCP addition. The decomposition peak of TLCP (around 517°C) appears when 25% TLCP is added.

The assumption of first order decomposition reaction enables us to calculate the thermal decomposition activation energy of the blends at the moment of initial decomposition. The weight loss rate per minute is

**Table 2** Dynamic thermogravimetric data of PEI/TLCP blends

| TLCP content (wt%) | Decomposition onset temperature (°C) | Maximum decomposition temperature (°C) | Activation energy, $E_a$ (kJ mol$^{-1}$) | log(pre-exponential factor), log($A$) (min$^{-1}$) |
|---|---|---|---|---|
| 0 | 496 | 555.0 | 207.5 | 11.90 |
| 5 | 492 | 553.5 | 196.0 | 11.31 |
| 10 | 485 | 544.2 | 231.0 | 13.91 |
| 25 | 485 | 518.0 | 284.9 | 17.59 |
| 50 | 474 | 515.6 | 284.4 | 17.82 |
| 75 | 478 | 514.9 | 321.0 | 20.45 |
| 100 | 477 | 520.8 | 283.0 | 17.72 |

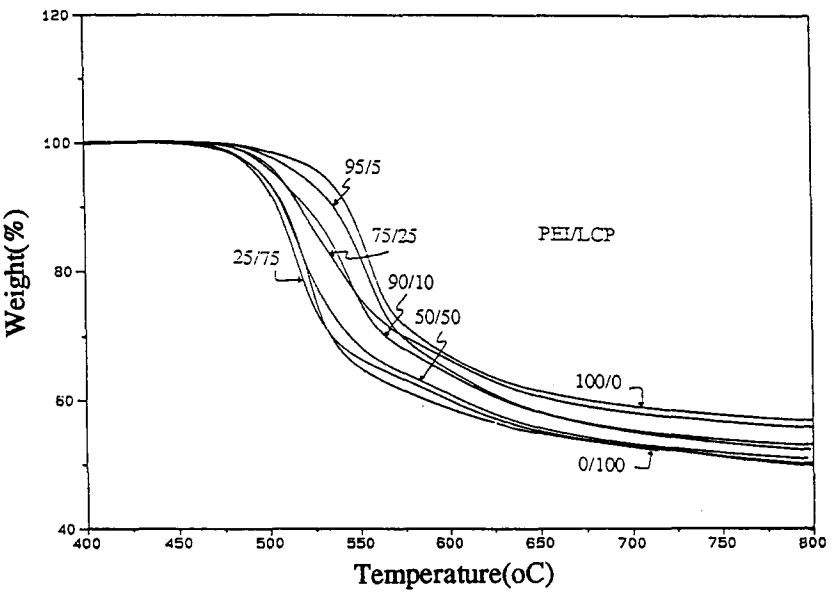


**Figure 2** T.g.a. thermograms of PEI/TLCP blends (heating rate 10°C min$^{-1}$)

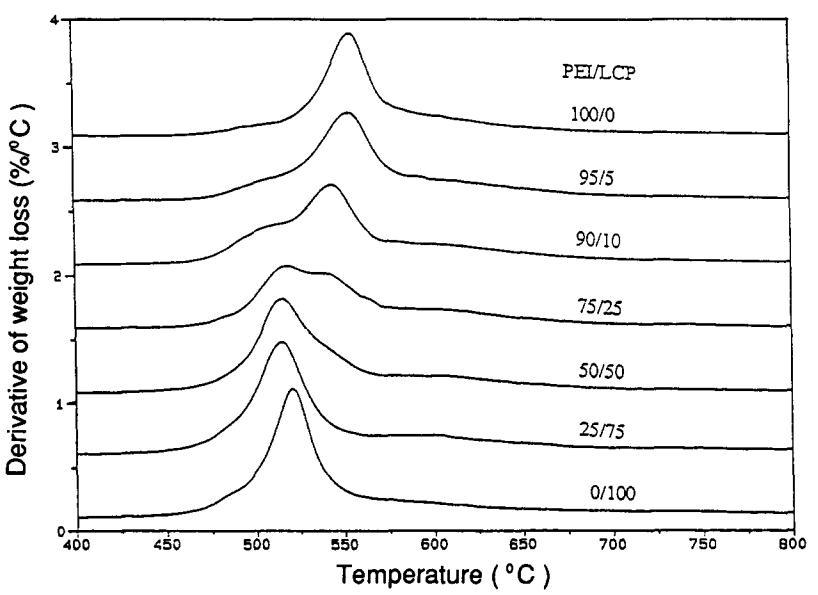


**Figure 3** Derivatives of weight loss with respect to temperature

represented as:

$$\frac{dW}{dt}=\left(\frac{dW}{dT}\right)\left(\frac{dT}{dt}\right)=k(W_d-W) \quad (1)$$

where $W$ is the weight loss at time $t$, $W_d$ is the weight loss at the final moment of the decomposition. $k$ is the reaction rate constant which can be expressed as an Arrhenius type function:

$$k=A\exp(-E_a/RT) \quad (2)$$

where $E_a$ is the activation energy of decomposition, $A$ is

the frequency factor and $R$ is the gas constant. From the plot of weight loss *versus* temperature, $E_a$ was calculated and is presented in *Table 2*. Although there is small deviation, the decomposition activation energy was about 210 kJ mol$^{-1}$ when the TLCP content was less than 25 wt%, and when the TLCP content was more than 25 wt%, it was about 285 kJ mol$^{-1}$. This shows that the PEI/TLCP blends have a synergistic effect on the retardation of thermal decomposition when TLCP content is low, but it also shows that blends have a synergistic effect on the acceleration of thermal decomposition when TLCP content is quite high; this is due to the thermal energy transfer between the matrix and dispersed phase. When the TLCP content is low, the thermal energy transfer to the dispersed TLCP phase should exceed the barrier of the thermally very stable PEI phase. On the other hand, when TLCP content is high, overcoming the energy barrier between different phases is easier due to the higher portion of TLCP. The frequency factor shows a similar behaviour.

*Rheological properties*

One of the principal factors that determines whether the dispersed phase forms elongated fibrils or is stabilized as droplets is the viscosity ratio. Many reports have observed that the viscosity of the TLCPs is lower than that of many engineering thermoplastics[1,2,6,22,23]. *Figure 4* shows the complex viscosity of PEI as a function of frequency at different temperatures. The general behaviour of PEI viscosity follows that of typical thermoplastic polymers, i.e. Newtonian behaviour at low shear rate and shear-thinning at high shear rate. The viscoelastic behaviour of Vectra B950 is not so simple. We measured viscoelastic properties for two samples. One was preheated to 340°C for 2 min then cooled to 180°C for 10 min. The other was not preheated. *Figure 5* shows the temperature dependence of the dynamic viscoelastic functions at low frequency. The viscosity of the preheated sample shows a drastic decrease over the temperature range of 290 to 310°C. The apparent activation energy calculated by plotting the viscosity *versus* $1/T$ at the temperatures is as high as 46 kcal mol$^{-1}$, suggesting a change in structure of the materials. The viscosity drop of the unpreheated sample is not so drastic. At high shear rates, preheated and unpreheated samples show almost the same behaviour; the viscosity decreases monotonically with temperature.

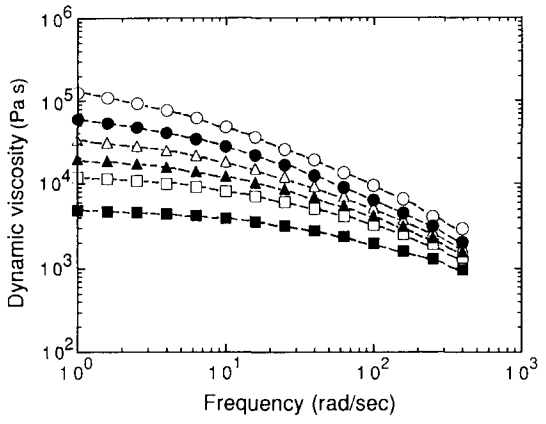


**Figure 4** Dynamic viscosity *versus* frequency for PEI at various temperatures: ○, 290°C; ●, 300°C; △, 310°C; ▲, 320°C; □, 330°C; ■, 340°C

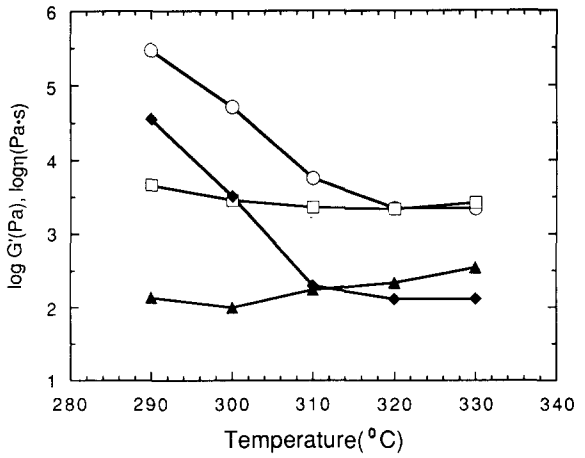


**Figure 5** Temperature dependence of dynamic viscoelastic functions at low frequency (0.1 rad s$^{-1}$): ○, viscosity for preheated sample; □, viscosity for unpreheated sample; ◆, $G'$ for preheated sample; ▲, $G'$ for unpreheated sample

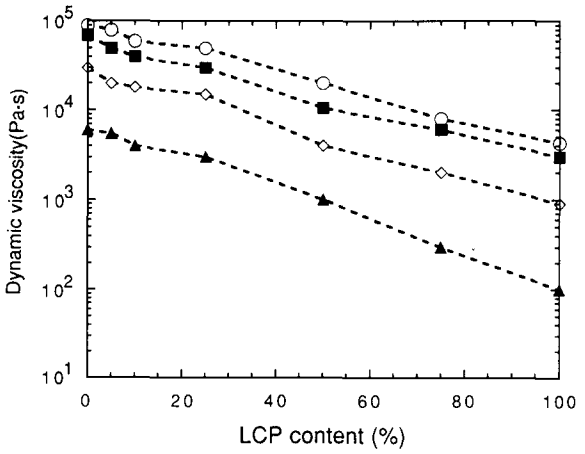


**Figure 6** Dynamic viscosity *versus* TLCP content for PEI/TLCP blends at 300°C: frequency rate: ○, 0.1 rad s$^{-1}$; ■, 1 rad s$^{-1}$; ◇, 10 rad s$^{-1}$; ▲, 100 rad s$^{-1}$

*Figure 6* shows the viscosity change *versus* TLCP content at 300°C. Viscosity drops with TLCP amount, which means that TLCP plays the role of a processing aid for the highly viscous PEI resin. The dynamic viscosity of the PEI/TLCP blends lies between those of the two resins. The structural change with more TLCP content in the blend reduces frequency dependence. The nematic crystalline formation temperature of Vectra B950 is 279°C. The distance between the crystalline phase increases at temperatures higher than the transition temperature, which reduces the interaction and changes the structure of the crystalline domain. This is similar to our previous observation on blends of poly(phenylene sulfide) and a TLCP (Vectra A900 from Hoechst Celanese)[24]. Since the viscosity of TLCP is lower than that of PEI in the entire temperature range, we expect that Vectra B950 easily forms fibrils in PEI.

Another rheological property, the storage modulus ($G'$) of the blends, shows a similar behaviour to blend viscosity. The storage modulus of pure TLCP samples behaves in the same manner as the viscosity shown in *Figure 5*. There is a rapid decrease of modulus at low temperature for the preheated sample, while at high temperature the decrease is not so significant. The unpreheated sample shows a complicated

phenomenon. At low temperature the modulus increases with temperature, but the opposite occurs at higher temperature, which is ascribed to the structural change. The rheological behaviour of Vectra B950 is more complicated than that of Vectra A900[26]. More details will be reported in the near future.

The storage modulus of the TLCP is lower than that of PEI. The $G'$ values of pure PEI and blends are shown in *Figures 7a* and *b*. $G'$ decreases with temperature. To observe the effect of temperature on the rheological properties of the blend, a logarithmic plot of storage modulus *versus* loss modulus ($G''$) of the blends, the so-called Cole–Cole plot, is used. This represents the elastic energy of the system plotted against the energy loss of the system. If the blend is totally compatible in all compositions, the curves will overlap to form one line. Also, from the time–temperature superposition principle, it is well known that no shift factor is required to obtain a master curve for quantities not including units of time. This implies that a plot of one such quantity *versus* another will be temperature-independent. For example, plots of $G'$ *versus* $G''$, with each point corresponding to a different frequency, are temperature invariant. This type of plot shows the relation between rheological properties and the molecular structure, such as molecular weight distribution and molecular weight, excluding the effect of processing variables.

*Figure 8* shows the modified Cole–Cole plot for the blends. Pure PEI shows a single master curve for all temperatures. Addition of TLCP causes the curve

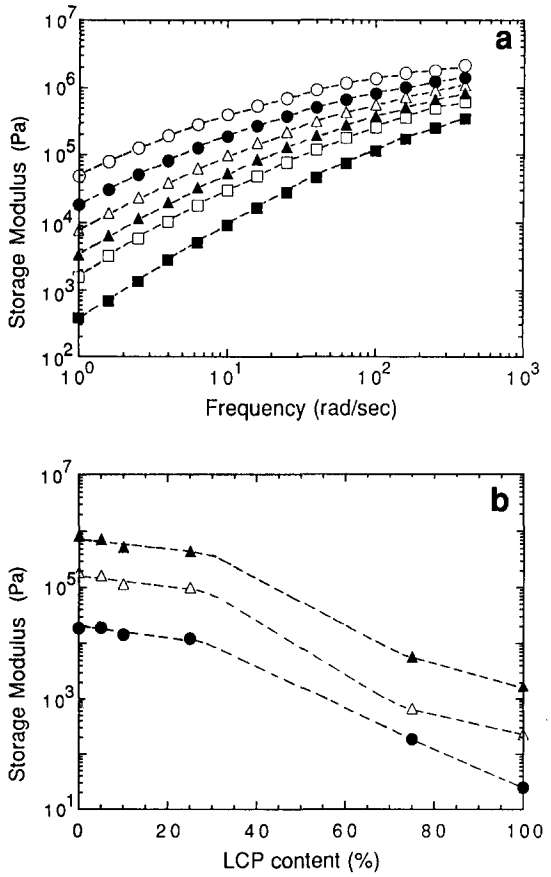


**Figure 7** (a) Storage modulus *versus* frequency for PEI at various temperatures: ○, 290°C; ●, 300°C, △, 310°C; ▲, 320°C; □, 330°C; ■, 340°C. (b) Storage modulus *versus* LCP content for PEI/TLCP blends at 320°C. Frequency: ●, 1 rad $s^{-1}$; △, 10 rad $s^{-1}$; ▲, 100 rad $s^{-1}$

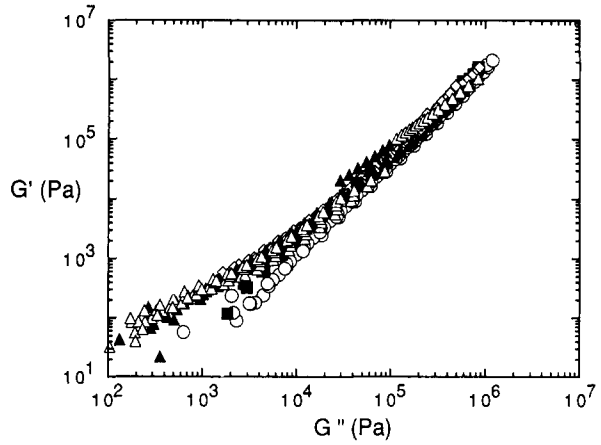


**Figure 8** Modified Cole–Cole plot for PEI/TLCP blends with different TLCP content: ○, 100/0; ■, 90/10; ◇, 75/25; ▲, 50/50; △, 25/75

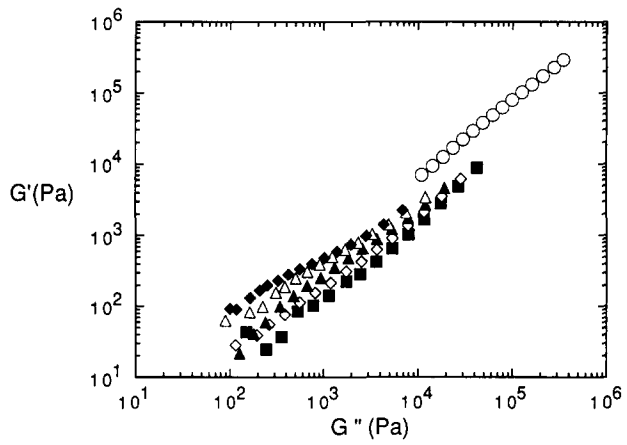


**Figure 9** Modified Cole–Cole plot of pure TLCP at different temperatures: ○, 290°C; ■, 300°C; ◇, 310°C; ▲, 320°C; △, 330°C; ◆, 340°C

to deviate from the linear relation. The effect of temperature is evident in the curves, because of the system's incompatibility. Addition of TLCP to pure PEI changes the homogeneous system to a non-homogeneous dispersed system. The TLCP domain is a rod shape which accepts shear orientation more easily to reduce the loss modulus. In *Figure 8*, the slope of pure PEI is close to 2, which agrees with the prediction of linear viscoelasticity. The slope deviates from the linear viscoelastic behaviour when more than 25% TLCP is added, which is due to the rod molecule's shear orientation. Also, the difference in the slope of the curve is seen at low and high values for PEI/TLCP blend compositions of 50/50 and 25/75: at low values (low frequency range) the respective slopes are about 0.5 and 0.4, but change to 1.2 and 1.4 at high values. This can be understood by looking at the modified Cole–Cole plot of pure TLCP presented in *Figure 9*. We can observe a similar behaviour of TLCP to that of the blends. However, the TLCP shape varies from crystallites to nematic state with increase in temperature. Due to this change, the TLCP blend deviates from single curve formation. High values correspond to 290°C, which is close to the crystal–nematic transition temperature. Around this temperature, some of the TLCP did not fully melt to form the isotropic liquid phase but remained in a non-isotropic rigid state in the form of deformable rigid particles. Increasing the temperature removes this

inhomogeneity and lends more fluidity. Therefore the effect of temperature appears in the curves that do not form a single curve.

*Mechanical properties*

The effect of the addition of Vectra B950 to PEI on tensile strength is shown in *Figure 10*. The processing temperature was 320°C. Tensile strength increased with TLCP content, as expected. More fibril formation occurs with higher draw ratio, which brings about the enhancement of tensile strength shown in *Figure 10*. Tensile strength increases rapidly at low draw ratio, but after a certain value of draw ratio it levels off. The more TLCP in the blend, the greater the effect of draw ratio on tensile strength. This finding is similar to a previous report[25].

Recently, Crevecoeur and Groeninckx[4] reported that in the blend system of TLCP (Ekonol E6000, a random copolyester from Sumitomo Chem.) and PEI (Ultem 1000), the modulus and tenacity of the system are independent of the draw ratio. They explained this as occurring because the reinforcing fibrils were formed mainly before and in the die, instead of beyond the die in the drawing step. Bassett and Yee[5] studied melt spun fibres of Vectra B950 and polystyrene; they also found little dependence of the modulus on the draw ratio for the blends, whereas the modulus of pure TLCP increased significantly with the draw ratio. However, Blizard *et al.*[22] reported that the modulus of strands of polycarbonate–Vectra blends increased with the draw ratio, and a plateau region for the modulus was not observed. In our system, the draw ratio effect is manifest at low draw ratio. Modulus and tensile strength are increased with draw ratio. The apparent dependence of modulus and strength on the draw ratio indicates that formation of reinforcing fibrils does not take place entirely in the die; it also takes place beyond the die exit in the drawing step. The orientation and texture upon exiting the extruder is complex because of the variation of flow field within the extruder and die exit. Within the extruder, the orientation of the nematic phase will vary from highly orientated at the walls to much less orientated at the centre. When the melt is hot drawn in an extensional flow field, the nematic domains are orientated in the direction of extrusion and appear to be drawn into orientated fibrils of high aspect ratio. After die exit, due to the matrix polymer's viscoelasticity, the composite fluid will be swollen. This extrudate swell will hinder heat transfer to the extrudate surface, which would give more fluidity. After the swelling region, the fluid will be in a strong elongational field where the disorganized portion of TLCP will be orientated in the flow direction. Hence the draw ratio effect will be manifest unless the drawing speed is so high that extrudate swell is negligible. For high TLCP content blends, swelling is not so great, but orientation of the fibril increases rapidly with draw ratio. After a certain draw ratio, most fibrils are in a perfectly orientated position to reach a constant plateau in modulus and strength. Therefore the major part of elongation and orientation of the TLCP, resulting in modulus improvement, is obviously obtained by the convergent flow through the spinneret at high draw ratio, but it is also partially ascribed to the subsequent drawing step beyond the die exit, especially at low draw ratio.

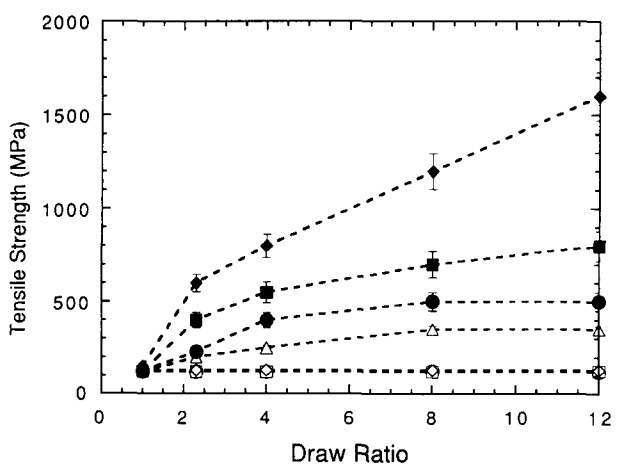


**Figure 10** Tensile strength *versus* spin draw ratio for PEI/TLCP blend fibres spun at 320°C: ◇, 100/0; □, 90/10; △, 75/25; ●, 50/50; ■, 25/75; ◆, 0/100

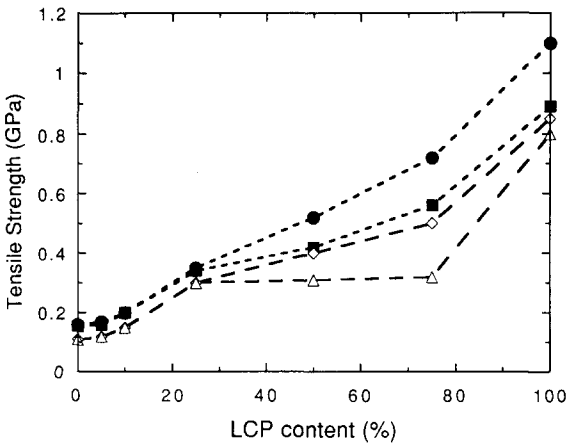


**Figure 11** Tensile strength *versus* TLCP content for PEI/TLCP blend fibres. Draw ratio = 4: ◇, spun at 320°C; △, spun at 340°. Draw ratio = 8: ●, spun at 320°C; ■, spun at 340°C

*Figure 11* shows the tensile strength *versus* TLCP content at draw ratios of 4 and 8. As seen in *Figure 10*, higher draw ratio provides higher tensile strength. Tensile strength increased remarkably when more than 25% TLCP was added. The tensile strength at 320°C is greater than at 340°C. This is because of the partial inhomogeneity, mentioned above. Sarlin *et al.*[28] reported similar results; they found that a polymer blend containing TLCP showed higher tensile strength when the processing temperature was greater than, but close to, the crystal–nematic transition temperature. This effect is more notable for blends with greater TLCP content. This is also due partly to the rheological behaviour of the blends. Two factors from the rheological point of view should be taken into consideration to obtain a polymer blend with good mechanical properties. The first is that the ratio of the viscosity of the dispersed phase to that of the matrix phase should be less than 1, but the second factor is that it should be close to 1 for good dispersion[29]. The viscosity of TLCP is much lower than that of PEI, as we have seen before. But the viscosity of TLCP is higher at lower temperature, which means that the blend processed at 320°C may have a more uniform dispersion than that processed at 340°C. This can be seen in the SEM photographs of the fracture surfaces of the fibres spun at the same draw ratio but at different

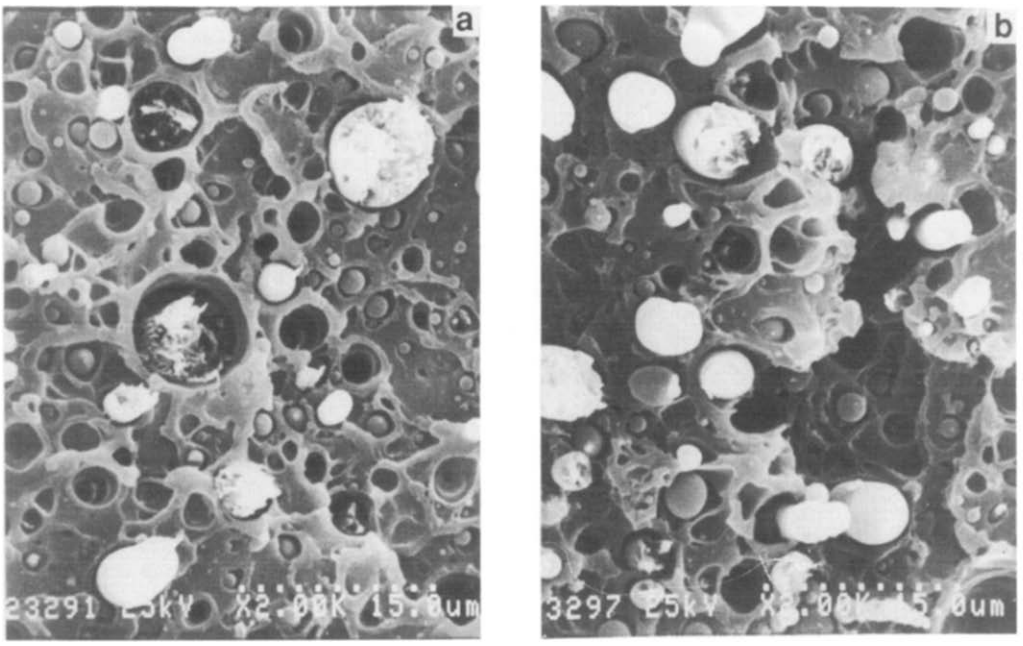


**Figure 12** SEM photographs of fractured surfaces of PEI/LCP blend fibres at a draw ratio of 1: (a) 320°C; (b) 340°C. Magnification 2000×

temperatures (*Figure 12*). TLCP domains spun at 320°C show more uniform dispersion. Further support comes from the fact that draw resonance of pure TLCP occurs more with extrusion at higher temperature. This agrees with other experiments on the mechanical properties of TLCP blends[23–25]. Another fact that should be mentioned regarding *Figure 11* is that the increase of tensile strength becomes less rapid when more than 50% TLCP is added at 340°C. This may be ascribed to the complex phenomenon of phase inversion, poor interface adhesion, unstable extension and non-uniform dispersion[30,31].

*Figure 13* shows the tensile modulus of the blends at the same draw ratios as *Figure 11*. It can be seen that molecular orientation at 320°C is better than at 340°C, which increases the tensile modulus. Molecular orientation can be conjectured from the aspect ratio of the fibre. Experimental observation of the aspect ratio of TLCP fibrils is quite difficult, if not impossible. However, the aspect ratio of the fibrils can be theoretically calculated from a modified Tsai–Halpin equation that has been applied by Nielson[32] to tensile strength calculation for fibre reinforced composite materials. The tensile modulus, $E$, of composite material can be expressed as:

$$\frac{E}{E_1}=\frac{(1+AB\phi_2)}{(1-B\phi_2)} \tag{3}$$

where $E_1$ is the tensile modulus of the matrix resin and $\phi_2$ is the volume fraction of the reinforcing fibre. Constant $B$ is represented as:

$$B=\frac{(E_2/E_1-1)}{(E_2/E_1+A)} \tag{4}$$

where $E_2$ is the fibre modulus. Constant $A$ depends upon the geometry of the composite formation. For axial direction under uniaxial orientation, it has the following form:

$$A=2(L/D) \tag{5}$$

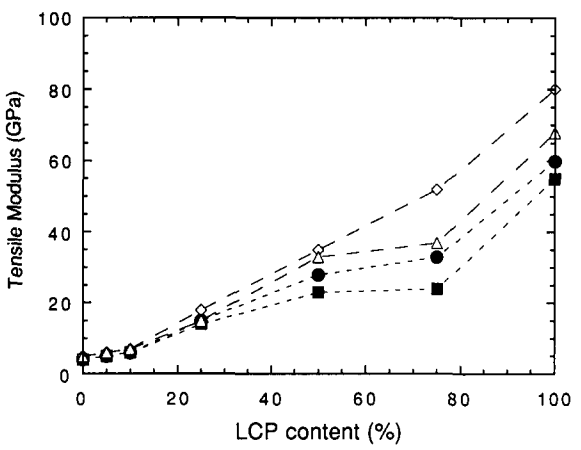


**Figure 13** Tensile modulus *versus* TLCP content for PEI/TLCP blend fibres. Draw ratio = 4: ●, spun at 320°C; ■, spun at 340°C. Draw ratio = 8: ◇, spun at 320°C; △, spun at 340°C

From equations (3), (4) and (5), we can calculate the aspect ratio if $E/E_1$ is provided for different fibril phase volume, $\phi_2$. *Figure 14* shows a graphical representation of the Tsai–Halpin equation with different aspect ratios at a draw ratio of 8. The rule of mixtures can be applied with large aspect ratios. The experimental values generally have a large aspect ratio when a large amount of TLCP (more than 25%) is added. *Figure 15* is a theoretical representation of equation (3) for tensile modulus *versus* aspect ratio with different TLCP volume contents. Tensile modulus rapidly increases at low aspect ratio, then levels off. A large TLCP volume content enhances the tensile modulus.

From *Figure 11* we can also see a rapid increase of tensile strength when 25% TLCP is added. The low aspect ratios for the 5 and 10 wt% TLCP composite fibres are ascribed to the low stiffness and low strength. The increase of aspect ratio, which means more fibril orientation with TLCP content, can be explained by the difference of TLCP particle size of different blends before they enter

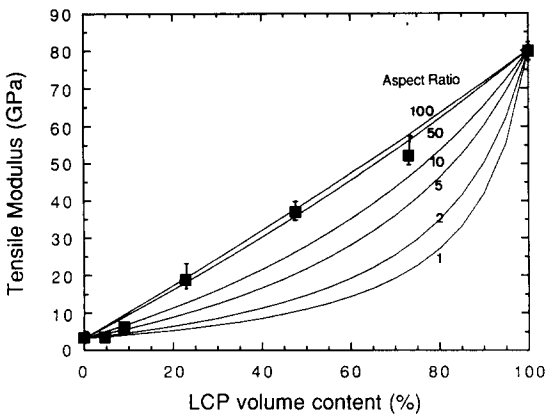


**Figure 14** Graphical representation of the Tsai–Halpin equation at a draw ratio of 8: ——, calculation; ■, experiment

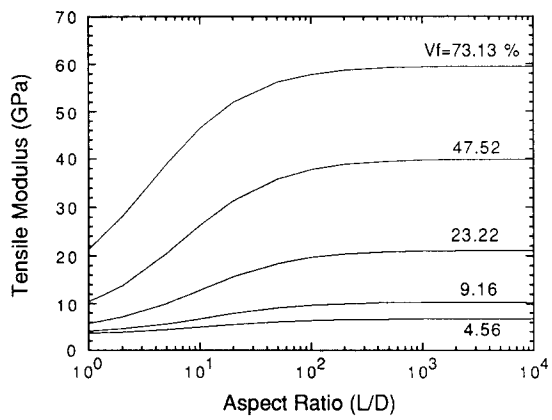


**Figure 15** Calculated tensile modulus as a function of aspect ratio for PEI/TLCP blend fibre at a draw ratio of 8 (Vf = volume fraction of TLCP)

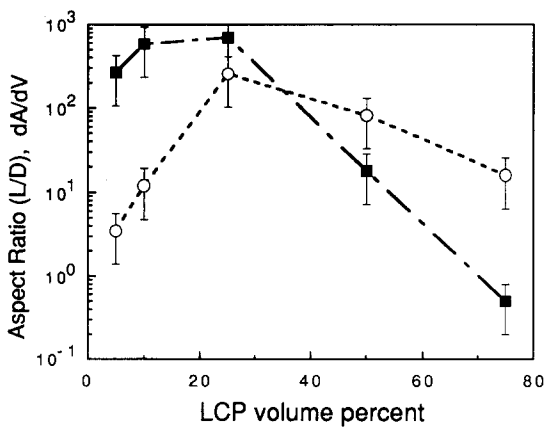


**Figure 16** Aspect ratio (○) and its derivative (■) *versus* TLCP volume content

the capillary. A smaller amount of TLCP in the blend will produce smaller particles. These smaller particles have a higher resistance to deformation due to surface tension[4]. For this reason, they will be elongated to a lesser extent, resulting in lower molecular orientation in the final TLCP fibrils. This is verified later by observation of their morphology.

The TLCP phase can form fibrillar shapes more easily with more TLCP because of easy orientation; however, too much TLCP prevents orientation because TLCP particles migrate to the high shear region. So there exists an optimum TLCP content for fibril formation. The theoretical value of aspect ratio as a function of TLCP volume content can be obtained from equations (3), (4) and (5). *Figure 16* is the calculated aspect ratio *versus* TLCP volume content. The maximum aspect ratio occurs at about 23 vol% TLCP, which is equal to 25 wt%. The maximum increase of aspect ratio ($dA/dV$) also takes place at 25 wt%. This agrees exactly with the experimental result. When more than 25 wt% TLCP is included, the fibrils are close to perfect orientation in the fibre direction. It is seen that the rule of mixtures can be conveniently applied for aspect ratios above 100.

*Morphology and property relation*

Improvement of tensile strength of the strands containing TLCP is due to the fact that the TLCP phase develops a fibrillar structure. This has been verified by SEM photographs. *Figure 17* shows SEM photographs of blend fibres spun at a draw ratio of 1. Vectra particles have been pulled out from the matrix during cryogenic fracture, indicating poor adhesion between the two phases. For the 75/25 PEI/TLCP blend (*Figure 17a*), a well dispersed TLCP phase is shown. However, many irregular fibrils with non-uniform domain size are seen in the 50/50 blend (*Figure 17b*). For the 25/75 blend, a different morphology appears (*Figure 17c*): the central portion looks the same as that of the 50/50 blend, i.e. non-uniform domain size, but the outer part clearly shows fibrils of the TLCP phase. This is the so-called 'skin–core morphology'. For pure TLCP (*Figure 17d*) the surface looks like the cross-section of a tree, with many coaxial layers. These photographs show that phase inversion occurred in the 50/50 blend.

*Figure 18* shows the effect of draw ratio for the 90/10 PEI/LCP blend. As expected, more orientation takes place at high draw ratio. At a low draw ratio of 1 (*Figure 18a*), the TLCP phase was slightly elongated but did not yet form fibrils. Some voids were formed after part of the TLCP phase was pulled out from the fractured surface. With higher draw ratio, the number of voids decreased whereas more fibrils began to develop. The diameter of the TLCP phase also varied: 1.2–1.5, 0.5–1 and 0.4 $\mu$m for draw ratios of 1, 4 and 8, respectively. The shape becomes more needle-like with increasing draw ratio. The photographs also show that a higher aspect ratio develops with increased draw ratio. This fibril formation at high draw ratio is because of the elongational energy transfer from highly viscous matrix polymer (PEI) to low viscous phase (TLCP) which is enough to elongate the dispersed phase.

In the previous section, we saw the effect of extrusion on the TLCP dispersion. The fibrillar morphologies in *Figure 12* also show that fibrils formed at 340°C are larger than those formed at 320°C. This can be surmised following the classic analysis of Taylor[33] on the average size of the dispersed particles, given by the relation:

$$R = \frac{C\sigma}{\dot{\gamma}\eta_m} \frac{16\frac{\eta_d}{\eta_m} + 16}{19\frac{\eta_d}{\eta_m} + 16} = \frac{C\sigma}{\dot{\gamma}\eta_m} F\left(\frac{\eta_d}{\eta_m}\right) \quad (6)$$

where $C$ is the apparent deformation (or the shape of the particles), $\dot{\gamma}$ is the shear rate, $\sigma$ is the interfacial tension and $\eta_d$ and $\eta_m$ are the viscosities of the dispersed phase and the matrix phase, respectively, in the processing

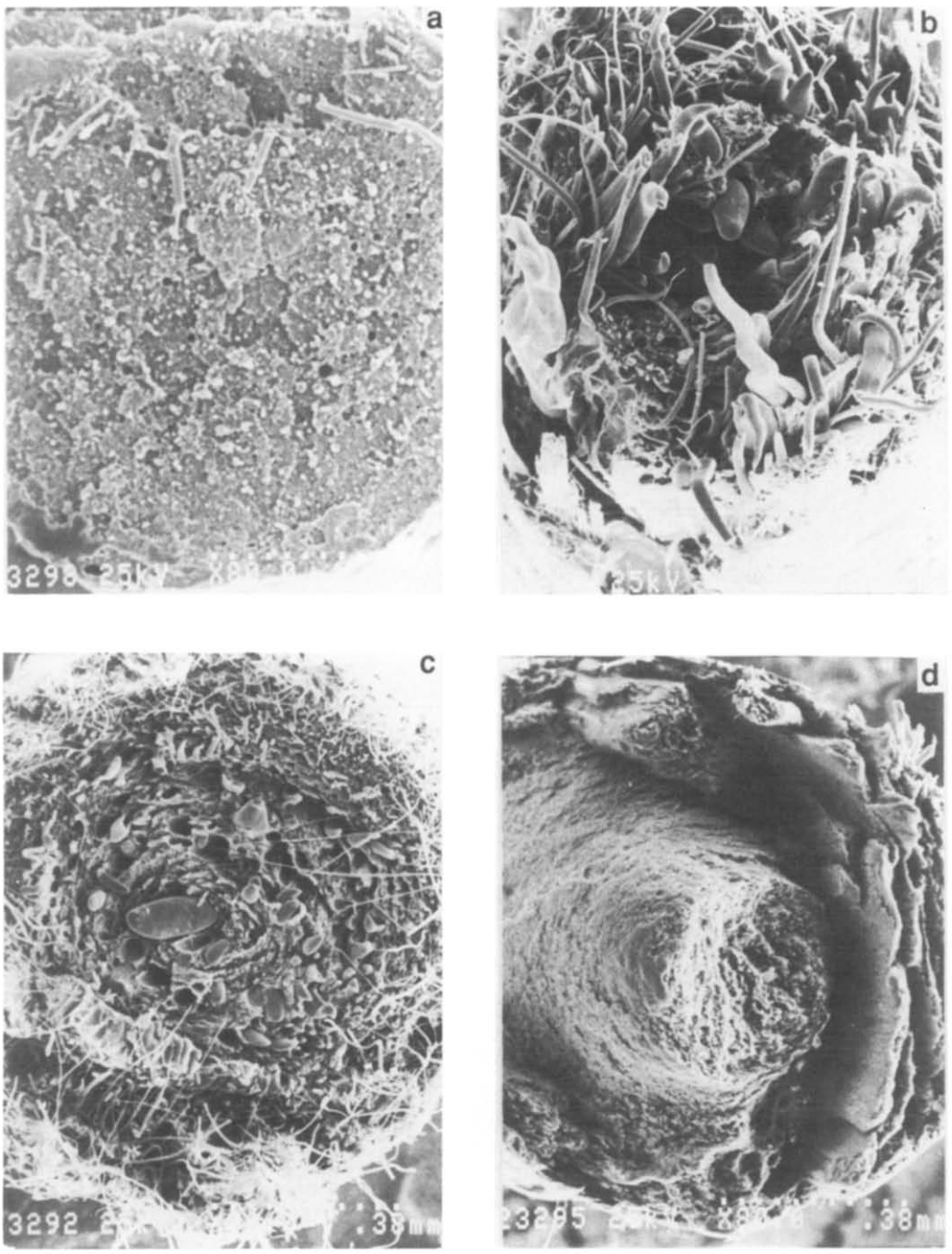


**Figure 17** SEM photographs of fractured surfaces of PEI/TLCP blend fibres spun at 320°C with a draw ratio of 1. (a) 75/25; (b) 50/50; (c) 25/75; (d) 0/100. Magnification 80×

conditions. By dividing the $R$ values at the two temperatures, assuming the same value of $\dot{\gamma}$ because the extrusions have been carried out at the same flow rate and the same $C$ values because in both cases the particles are broken, the ratio is represented as:

$$\tilde{R}=\frac{R^{340}}{R^{320}}=\frac{\sigma^{340}\eta_m^{320}}{\sigma^{320}\eta_m^{340}}\frac{\left[F\left(\frac{\eta_d}{\eta_m}\right)\right]^{340}}{\left[F\left(\frac{\eta_d}{\eta_m}\right)\right]^{320}} \quad (7)$$

Considering also that the interfacial tension is only slightly different in this temperature range[34] and the viscosity of the dispersed phase is two orders of magnitude smaller than that of the matrix at these temperatures, $R$ is just the inverse of the viscosity ratio at two temperatures, which is greater than 1. This means that larger particles of the dispersed phase are formed during extrusion at higher temperature. This agrees with the morphology of the fibres shown in *Figure 12*. During flow in the converging die, the particles of the liquid crystalline polymer are elongated[35]. Then the dimensions of the fibre orientated at 340°C, coming from larger particles, are greater than those of fibres obtained at 320°C, as shown in *Figure 12*.

*Figure 19* shows SEM photographs of fractured surfaces of composite fibres with different TLCP contents. As mentioned above, the more TLCP is included, the larger the particle. This helps easy deformation under the flow field due to low surface tension by larger curvature. As a result, it produces more orientated fibrils.

Crystalline fibril formation can be confirmed by wide

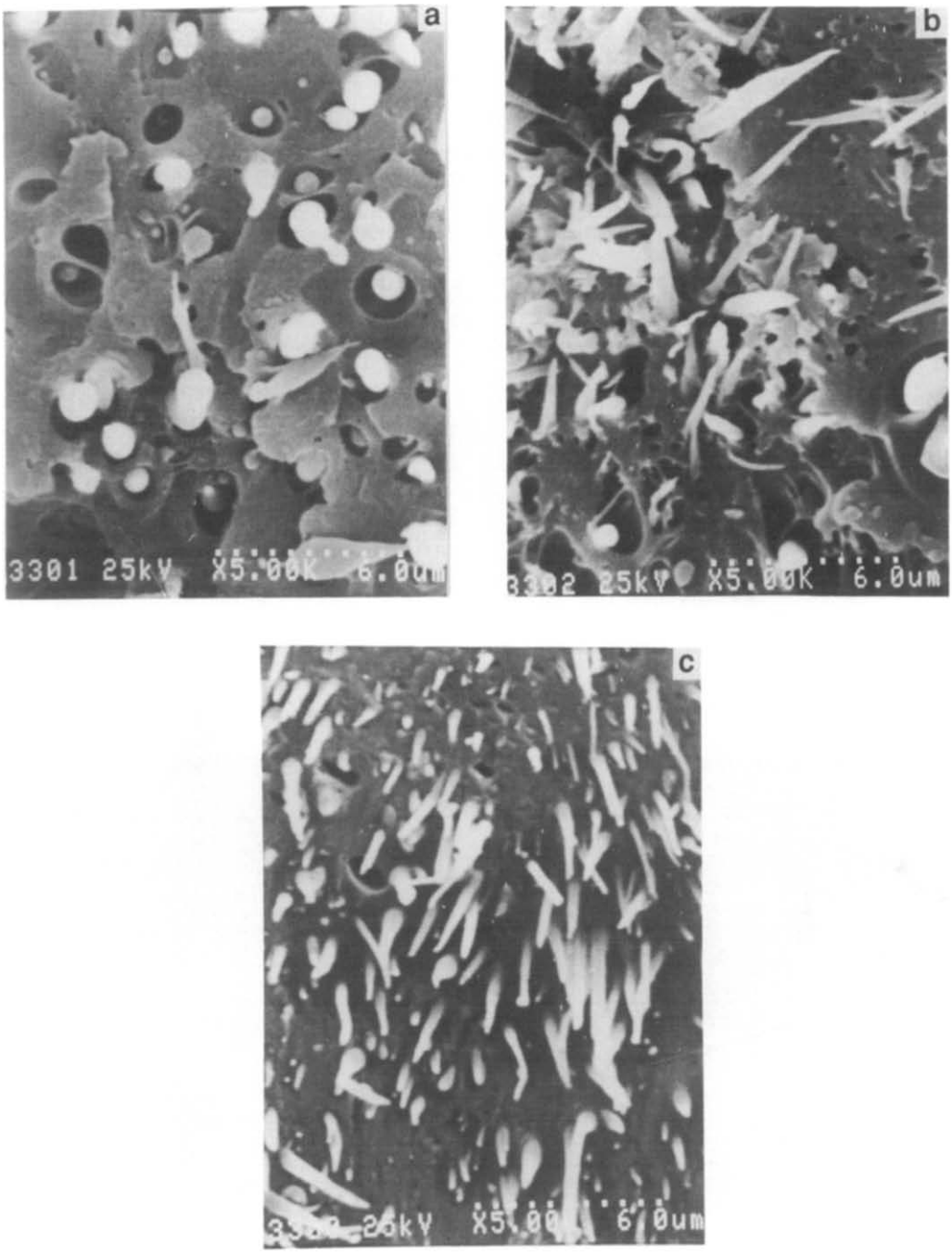


**Figure 18** SEM photographs of fractured surfaces of PEI/TLCP blend fibres spun at 320°C with different draw ratios: (a) 1; (b) 4; (c) 8. Magnification 5000 ×

angle X-ray diffraction (WAXD). *Figure 20* shows different WAXD patterns. At low draw ratio, an amorphous ring can be clearly seen (*Figure 20a*), but it is reduced with high draw ratio (*Figure 20b*). On the other hand, highly non-isotropic crystalline and fibril orientation are observed in high draw ratio strands. More details about the structure of the blended fibres will be reported in the future.

## CONCLUSIONS

Blends of PEI (Ultem 1000) with TLCP (Vectra B950) were studied. Strands were extruded and their properties were examined. Since these two polymers are incompatible, their behaviour, in general, follows that of incompatible polymer blends. The study of thermal properties revealed that the $T_g$ of the blends was decreased with increasing TLCP content, and stability at high temperature was also decreased. Viscosities of the blends were placed between those of PEI and TLCP, which supported the idea that TLCP molecules might be able to aid processing due to low viscosity at a temperature higher than the liquid crystalline formation temperature. The tensile strength and tensile modulus of the blends were increased with TLCP content. The draw ratio effect was clearly shown with more TLCP content. The tensile strength at 320°C was higher than at 340°C since the blend had better dispersion when the processing temperature above the crystal–nematic transition temperature was close to the transition temperature. The blend showed maximum aspect ratio when the TLCP content was 25 wt%. This agrees with theoretical calculation using the Tsai–Halpin

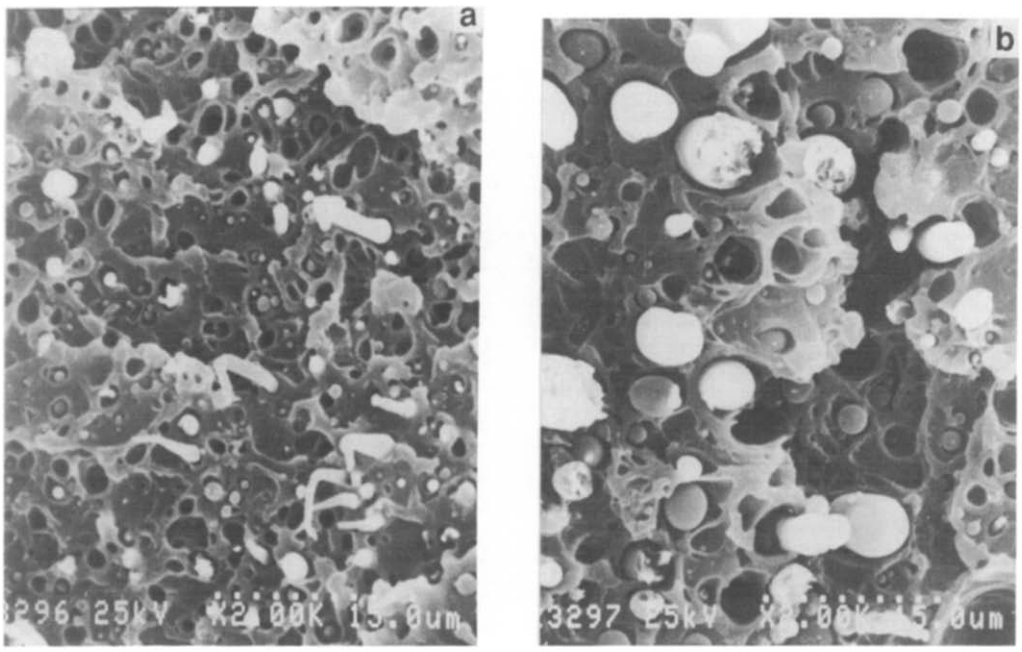


**Figure 19** SEM photographs of fractured surfaces of PEI/TLCP blend fibres spun at 340°C with a draw ratio of 1: (a) 90/10; (b) 75/25. Magnification 2000 ×

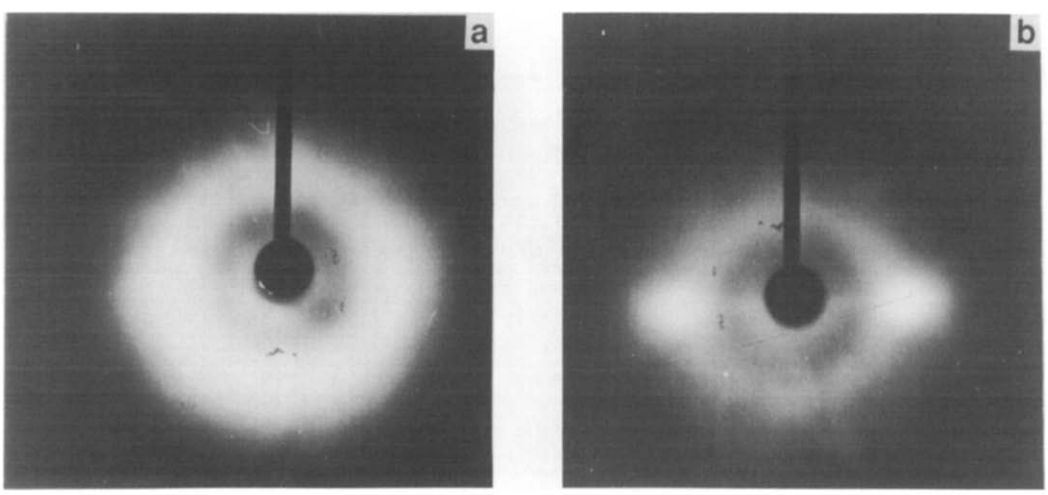


**Figure 20** Wide angle X-ray diffraction patterns of 75/25 PEI/TLCP blend fibres spun at 320°C with different draw ratios: (a) 1; (b) 8

equation. TLCP orientation and steric effect induce the optimum TLCP amount for fibril formation. It also emphasizes the fact that a certain minimum composition of the reinforcing TLCP phase must be present for the formation of fibrils. Surface photographs by SEM are in agreement with previous results and WAXD photographs show that high draw ratio enhances fibril formation.

The PEI and TLCP used in this study are immiscible. Partial miscibility of the dispersed phase with the matrix can bring about many property changes, including fibril generation. We feel that this should be examined further to improve the mechanical properties of the PEI/TLCP system. We can apply two different methods for this purpose. The first is functionalization at the dispersed phase surface, and the second is the addition of the compatibilizer. This study is under way and will be reported in the near future.

## REFERENCES

1 Mithal, A. K., Tayebi, A. and Lin, C. H. *Polym. Eng. Sci.* 1991, **31**, 1533
2 Prevorsek, D. C. in 'Polymer Liquid Crystals' (Eds A. Cifferi, W. R. Krigbaum and R. B. Meyer), Academic Press, New York, 1982, pp. 329–376
3 Weiss, R. A., Huh, W. and Nicolais, N. *Polym. Eng. Sci.* 1987, **27**, 684
4 Crevecoeur, G. and Groeninckx, G. *Polym. Eng. Sci.* 1990, **30**, 532
5 Bassett, B. R. and Yee, A. F. *Polym. Compos.* 1990, **11**, 10
6 Isayev, A. I. and Modic, M. *Polym. Compos.* 1987, **8**, 158
7 Jung, S. H. and Kim, S. C. *Polym. J.* 1988, **20**, 73
8 Acierno, D., Amendola, E., Carfargna, C., Nicolais, L. and Nobile, R. *Mol. Cryst. Liq. Cryst.* 1987, **153**, 553
9 Nobile, M. R., Amendola, E., Nicolais, L., Acierno, D. and Carfargna, C. *Polym. Eng. Sci.* 1988, **29**, 224
10 Malik, T. M., Carreau, P. J. and Chapleau, N. *Polym. Eng. Sci.* 1989, **29**, 600
11 Kohli, A., Chang, N. and Weiss, R. A. *Polym. Eng. Sci.* 1989, **29**, 573

12 Shin, B. Y. and Chung, I. J. *Polym. J.* 1989, **21**, 851
13 Kiss, G. *Polym. Eng. Sci.* 1987, **27**, 420
14 James, S. G. and Donald, A. M. *Mol. Cryst. Liq. Cryst.* 1987, **153**, 501
15 Siegman, A., Dagan, A. and Kenzig, S. *Polymer* 1985, **26**, 1325
16 Chung, T. S. *Plast. Eng.* 1987, (October), 39
17 Shin, B. Y. and Chung, I. J. *Polym. Eng. Sci.* 1990, **30**, 22
18 La Mantia, F. P., Valenza, A., Paci, M. and Magagnini, P. L. *Polym. Eng. Sci.* 1990, **30**, 7
19 Bristow, W., Dziemianowicz, T. S., Romanski, J. and Weber, W. *Polym. Eng. Sci.* 1988, **28**, 785
20 Ko, C. U. and Wilkes, G. L. *J. Appl. Polym. Sci.* 1989, **37**, 3063
21 Sukhadia, A. M., Done, D. and Baird, D. G. *Polym. Eng. Sci.* 1990, **30**, 519
22 Blizard, K. G., Sukhadia, A. M., D'Souza, P. and Baird, D. G. *Polym. News* 1990, **15**, 307
23 Hong, S. M., Kim, B. C., Kim, K. U. and Chung, I. J. *Polym. J.* 1991, **23**, 1347
24 Hong, S. M., Kim, B. C., Kim, K. U. and Chung, I. J. *Polym. J.* 1992, **24**, 727
25 Hong, S. M., Kim, B. C., Kim, K. U. and Hwang, S. S. *Polym. Eng. Sci.* 1993, **33**, 630
26 Lin, Y. G. and Winter, H. H. *Macromolecules* 1991, **24**, 2877
27 Calahorra, M. E., Equizabal, J. I., Cortazar, M. and Guzman, G. M. *Polym. Commun.* 1987, **28**, 39
28 Sarlin, J. and Tormala, D. *J. Appl. Polym. Sci.* 1990, **40**, 453
29 Wu, S. *Polymer* 1985, **26**, 1855
30 Massakazu, I., Kuniaki, A., Yasuro, S. and Hiroaki, S. European Patent 0 261 869, 1987
31 Oyanagi, Y. *Plastic Mold. Tech.* 1987, **4**, 89
32 Nielson, L. E. 'Mechanical Properties of Polymers and Composites', Marcel Dekker, New York, 1975, p. 379
33 Taylor, G. I. *Proc. R. Soc. Ser. A* 1934, **146**, 501
34 Wu, S. 'Polymer Interface and Adhesion', Marcel Dekker, New York, 1982
35 Garg, S. K. and Kenig, S. in 'High Modulus Polymers' (Eds A. E. Zachariades and R. S. Porter), Marcel Dekker, New York, 1988, Ch. 3